

AST325 Lab 1

Shimona Das

September 2024

Abstract

Complementary Metal-Oxide-Semiconductor (CMOS) cameras are light sensitive devices made up of pixel arrays that convert incident light into electrical signals using photo-generated electrons which enables the detection and mapping of light intensity. In this experiment, a Point Grey FMVU-03MTM-CS CMOS detector was used and its gain, read noise, and dark current was analysed. Using photon count data, the relationship between mean pixel intensity and variance was investigated, revealing a gain of approximately $1019.9 \times 10^{-4} \pm 45.9$ e-/ADU, read noise of $0.34 \pm 1 \times 10^{-4}$ ADU and a dark current of 28.9 ± 0.1 e-/sec/pixel. The detector's response to varying photon count rates was examined, confirming that it follows Poisson statistics at lower signal levels but exhibits saturation effects at higher intensities. Dark current was then measured by observing the linear accumulation of thermally generated electrons over time. These findings provide insights into the detector's performance, especially for low light and long exposure applications which emphasises the importance of noise correction techniques in scientific imaging.

1 Introduction

The detection and characterization of light is a fundamental part of many areas of scientific research, including astronomy, biology, and physics. Modern detectors such as Charge-Coupled Devices (CCDs) and Complementary Metal-Oxide-Semiconductor (CMOS) sensors have revolutionized imaging by allowing precise measurements of light all the way down to the individual photon level. These detectors convert incident photons into electrical signals, which are then digitized into measurable units known as Analog-to-Digital Units (ADUs). However, in order to extract meaningful data from these sensors, it is important to understand the inherent noise present in the system such as dark current and read noise, and to calibrate the detector to convert the digital output into physical units, such as the number of electrons generated per photon.

In this experiment, the noise characteristics and performance of a Point Grey FMVU-03MTM-CS CMOS detector was investigated. The detector's sensitivity to light and noise, as well as its gain (the conversion factor between ADU and electrons), are metrics that allow the understanding of how well it can detect

low-intensity signals and accurately measure light in varying conditions at different settings. To accomplish this, the mean pixel intensity and variance was measured in the detector's output, both under light and dark conditions. By analyzing the relationship between the mean pixel intensity and the variance, the detector's gain and read noise was determined. Additionally, by measuring dark frames (frames taken without any light) the dark current of the detector was quantified which comes from thermally generated electrons accumulating in the sensor over time.

Dark current is an important source of noise, especially in long-exposure imaging because it adds to the overall signal measured by the detector even in the absence of light. This noise must be carefully measured and subtracted from the data to ensure accurate results. The study of noise in this experiment, specifically read noise and dark current, provides insights into the detector's performance in real world applications where minimizing and correcting for noise is crucial for accurate measurements. This report begins by describing the experimental setup and the data collection methods. The primary focus is on understanding how dark current and read noise affect the detector's performance, and how these parameters were measured. The data reduction techniques used to clean and process the raw data are then discussed, followed by an analysis of the results, where we calculate the gain, read noise, and dark current of the detector. The report concludes with a discussion of the significance of these findings and their broader implications for the use of CMOS detectors in scientific imaging.

2 Data and Observation

Specification	CMOS
Sensor type	1/3 inch
Model	Micron MT9V022 CMOS
Imaging Mode	Colour (RGB)
Pixels count	752×480 - 0.3 Mp
Pixel size	6.0 m
Digitization	10-bit(8-bits are used)
Gain Range	0 - 12 dB

Table 1: Properties of CMOS (FMVU-03MTM-CS)

Date	Personnel	Notes
13/09/2021	S. Das, M. Pye, J. Hora	Set up and investigate live view window.
20/09/2021	S. Das, M. Pye, J. Hora	Examined the histogram for various settings.
27/09/2021	S. Das, M. Pye, J. Hora	Measured read noise and dark current.

Table 2: A summary of observations

Frame Type	Exposure Time (ms)	Mean Photon Count (ADU)	Standard Deviation (ADU)
Dark	0.06 - 30	5 - 15	2.3
Light	0.06 - 30	180 - 220	20.1

Table 3: Summary of data collected during the experiment, including the exposure time and statistical properties of photon counts for dark and light frames for 30 frames and a gain of 12 dB.

Exposure Time (ms)	Mean Value (ADU)
1	9.06
5	9.21
10	9.36
15	9.50
20	9.68
25	9.84
30	9.95

Table 4: Dark Frame Collection: Mean pixel values measured across various exposure times using the Point CMOS detector. The dark frames were collected with the lens cap on to capture the inherent noise of the detector, including dark current and read noise. The exposure times ranged from 1 ms to 30 ms, with a fixed gain of 12 dB, a brightness setting of 146, and a frame rate of 30 fps. As expected, the mean values slightly increased with longer exposure times due to the accumulation of dark current, which is a function of thermal excitation in the detector.



(a) Side view of CMOS camera



(b) Rear view of CMOS camera

Figure 1: (a) The Point Grey FMVU-03MTM-CS CMOS detector setup used to capture photon intensity measurements. (b) Rear view of the same CMOS detector showing the serial number and connectivity.

As shown in Figure 1, the experiment involved systematically adjusting the camera's settings to collect data under various conditions. For the first part of the experiment, the shutter speed of the CMOS detector was varied between 0.062 ms and 11.308 ms. When the shutter was set to 0.062 ms, the histogram of pixel intensities displayed a mean of approximately 9 ADU, with a maximum around 24 ADU and a range at 0 ADU. As the exposure time increased to 11.308 ms, the mean gradually rose to 255 ADU, with both the minimum and maximum values also reaching 255 ADU, indicating that the camera's dynamic range had been fully utilized. Beyond this, while the maximum value remained constant, the minimum values occasionally dropped to zero. Following this, the camera's lens cap was placed on to capture dark frames, and the frame rate was alternated. The lowest frame rate used was 4.61 Hz and the highest was 30.43 Hz. Next, the camera was mounted on a box and directed towards a plain whiteboard, a uniform source, to examine the histogram's characteristics under uniform illumination. The same procedure was repeated with a non-uniform source, a patterned pencil pouch, to observe the differences in pixel intensity distribution. To measure the read noise, the camera was pointed at a scene with both bright and dim regions. The settings were adjusted so that the dimmer regions approached zero signal (0 ADU), while the brighter regions were close to saturation (255 ADU). A series of 20-30 images were then collected, and these images were later analyzed to calculate key performance metrics of the detector, such as the gain, read noise, and dark current.

3 Data Reduction

The data reduction process in this experiment involved several steps aimed at cleaning and preparing the raw data for scientific analysis. Each step was designed to minimize the influence of noise and ensure that the data reflected the true signal generated by photon detection. The main focus was on dark frame subtraction, mean and variance calculations. The first step in the data reduction process was dark frame subtraction. Dark frames were captured with the lens cap on, which allowed the measurement of the inherent noise of the detector, such as dark current and read noise, without any contribution from external light sources. Dark current's effects grow with longer exposure times, introducing additional Poisson noise. By averaging the dark frames (as shown in Table 4) and subtracting the resulting averaged dark frame from each light frame, we were able to correct for these noise contributions. This method is important because it isolates the photon signal from systematic noise introduced by the detector itself, improving the accuracy of the measurements.

After subtracting the dark frames, the next step was to compute the mean and variance of each pixel across all the corrected light frames. This analysis is crucial because it provides insight into the statistical behavior of the detector, particularly in the context of Poisson statistics, where the variance is expected to scale with the mean. By calculating the mean pixel intensity and the corresponding variance for each pixel, the relationship between these two quantities

was assessed. The result was a scatter plot of mean vs the variance, which was used to determine the gain and noise characteristics of the detector. The gain is derived from the inverse of the slope of the linear fit, while the intercept represents the read noise, which is the baseline noise introduced by the camera. In terms of uncertainty, this was a key consideration throughout the data reduction process. The subtraction of the averaged dark frame significantly reduced uncertainty by accounting for noise due to dark current and thermal excitation. In addition, it was assumed that Poisson noise was the dominant source of statistical variation in the light frames. This explains the linear relationship observed between the mean and variance. The presence of read noise was also considered, which is why the intercept of the linear fit was not zero. This read noise quantifies the uncertainty introduced by the camera electronics, even when no photons are detected.

During data collection, some fluctuations in the dark frame pixel values at higher exposure times were encountered, as mentioned in Section 2. These fluctuations were likely due to minor temperature changes and electronic noise within the detector. While the fluctuations were small, they introduced some uncertainty into the dark frame data. However, we determined that these variations were not significant enough to reject any of the data. The motivation for this data reduction process was to ensure that the raw data was cleaned of any systematic noise. Dark frame subtraction is a standard technique in image processing, especially in astronomy, to correct for noise from thermal excitation in the detector. The calculation of pixel-wise mean and variance allowed us to evaluate the detector's performance, particularly its gain and noise characteristics. By systematically reducing the data, we were able to generate a clean dataset that accurately represented the true signal from the photons being detected.

Overall, the data reduction process played a crucial role in transforming the raw data into a usable format for analysis. The result of this process is the linear relationship between mean and variance, as seen in Figure ??, which highlights the effectiveness of the noise correction techniques and the accuracy of the data reduction.

4 Data Analysis

The analysis of the data collected in this experiment is presented through various plots that provide valuable insights into the performance of the CMOS detector. These plots were generated to investigate the photon count rates and assess the detector's response under various conditions. This section explores these plots and their corresponding interpretations.

The first plot in the analysis is a histogram which compares photon count rates to an expected Poisson distribution. The photon count rates measured in the experiment closely follow the Poisson distribution with a mean of 12 photons per second. As seen in Figure 1, the histogram shows the distribution of photon count rates over several measurements, while the dashed line represents the expected Poisson distribution. The data matches the Poisson curve quite well,

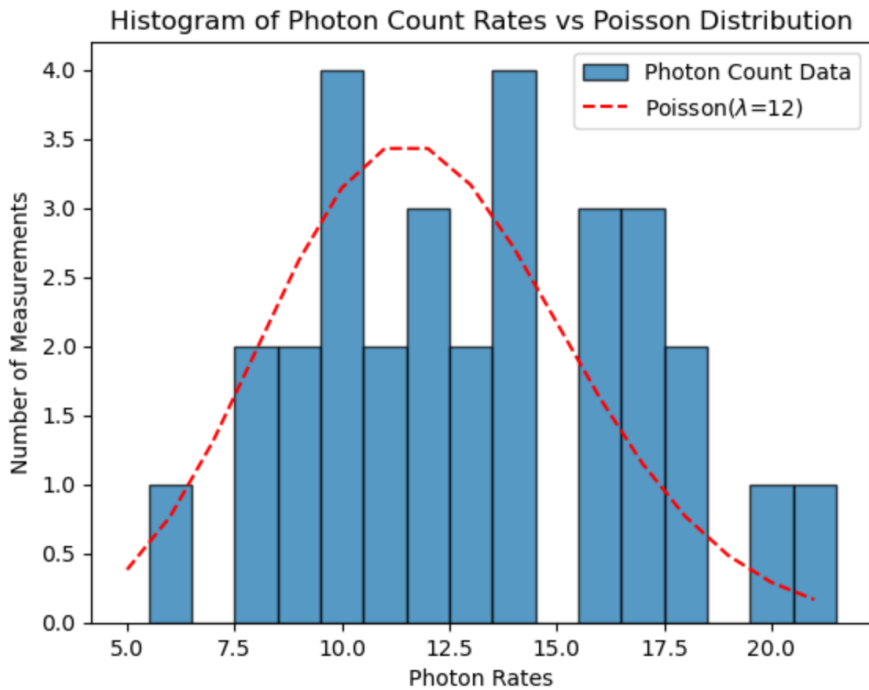


Figure 2: Histogram of photon count rates overlaid with the expected Poisson distribution . The blue bars represent the frequency of measured photon rates, while the red dashed line represents the Poisson distribution fit. This comparison highlights how well the photon count data follows a Poisson distribution, which is characteristic of photon-counting systems where the events follow a random process. The match between the data and the Poisson distribution supports the theoretical expectation of photon arrival being governed by Poisson statistics.

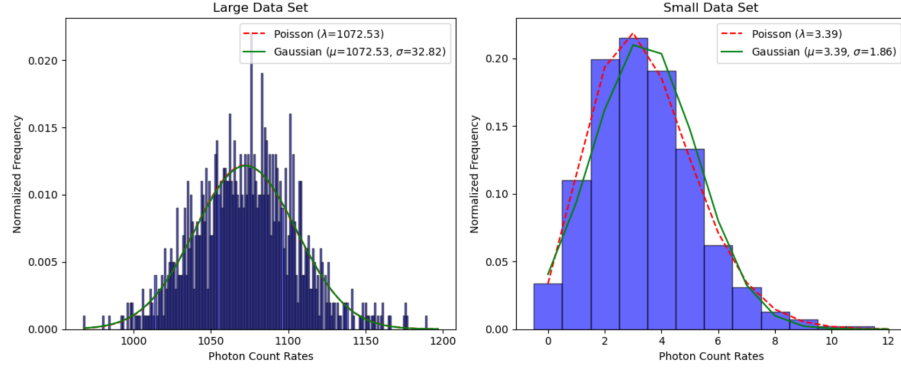


Figure 3: Histograms of photon count rates for the "Large" (left) and "Small" (right) datasets overlaid with Poisson and Gaussian distributions. The "Large" dataset (mean = 1072.53, standard deviation = 32.82) is well-approximated by both the Poisson (red dashed line) and Gaussian (green solid line) distributions, demonstrating the convergence of Poisson to Gaussian behavior at high mean photon count rates. The "Small" dataset (mean = 3.39, standard deviation = 1.86), however, follows the Poisson distribution more closely, as expected for lower photon count rates where the asymmetry of the Poisson distribution is more pronounced.

particularly in the middle range, which confirms that photon detection by the camera follows the expected Poisson statistics. At the extremes, the deviations from the Poisson curve are likely due to fluctuations in the photon detection process, which are captured by the inherent noise in the detector.

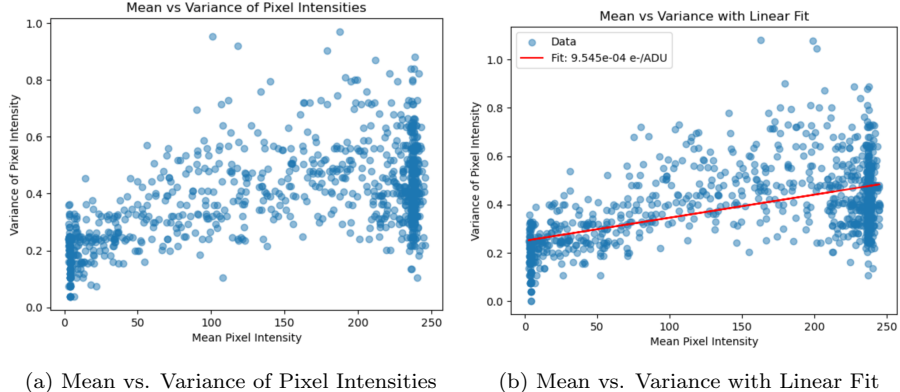
Next, it is examined whether the calculated values for both the "Large" and "Small" datasets are consistent with what we expect from a Poisson distribution. The "Small" dataset, with a mean photon count rate of 3.39 and a standard deviation of 1.86, fits a Poisson distribution almost perfectly, as evidenced by the histogram and the overlaid Poisson fit (red dashed line). The Poisson distribution accurately captures the asymmetric nature of the data for smaller mean values, consistent with what we expect. On the other hand, for the "Large" dataset, where the mean photon count rate is much higher (1072.53) along with the standard deviation (32.81), the Poisson distribution starts resembling a Gaussian distribution, which is expected when photon count rate is large due to the convergence of the Poisson distribution to a normal distribution according to the Central Limit Theorem. Hence, both datasets exhibit behaviors consistent with Poisson statistics, but the "Large" dataset is better modeled by a Gaussian distribution because of the high photon count rate.

In terms of the camera's performance, significant variations were observed based on shutter speed, exposure time, and aperture size, which are crucial for understanding the system's noise behavior. For instance, while observing the live display and the histogram tool, the maximum data value returned by the

camera was recorded at a mean value of 255 ADU at 11.308 ms, where both the minimum and maximum values remained fixed at 255. This indicates that the camera reaches its full dynamic range at longer exposure times. In contrast, at 0.062 ms, the histogram mean was around 9 ADU, with a maximum of 24 ADU, showing how exposure time directly impacts the mean pixel intensity.

The live view window, when the lens cap was placed on the camera, showed that as exposure time increased, the image became brighter and less noisy, particularly at lower frame rates. The lowest frame rate was observed to be 4.61 Hz, while the highest frame rate was 30.43 Hz. At shorter shutter speeds, such as 0.062 ms, the mean value was 54.77 ADU (green channel), with a min of 39 ADU and a max of 170 ADU. As the exposure time increased to 355.855 ms, the mean increased to 60.23 ADU, indicating a gradual increase in brightness and pixel values. However, the fluctuations in the min and max values (from 42 to 223) reflect noise variations as exposure time increases.

Additionally, pointing the camera at the uniform target (whiteboard) highlighted the effect of aperture size on the histogram. At the largest aperture ($F/1.4$), the mean value was 215 ADU, with a wide histogram spread and low peak, indicating a significant variation in brightness across the image. This suggests a higher noise level when the aperture is fully open. In contrast, at the smallest aperture ($F/8$), the mean value dropped to 12.87 ADU, with a much narrower histogram peak. This suggests a more uniform distribution of pixel intensities at lower light levels, which is expected as a smaller aperture reduces the amount of light entering the camera. When pointed at a non-uniform source, the histogram of pixel intensities showed a broader spread due to the varying brightness levels across different parts of the image. This resulted in a higher standard deviation reflecting greater variation. With auto-exposure is on, the camera adjusted dynamically, further affecting the histogram.



(a) Mean vs. Variance of Pixel Intensities

(b) Mean vs. Variance with Linear Fit

Figure 4: (a) shows the relationship between the mean pixel intensity and variance of pixel intensities. This scatter plot reveals a clear positive correlation, which is expected due to the nature of photon noise governed by Poisson statistics. In photon-counting systems, the variance is expected to grow proportionally with the mean, and this trend is evident in the data. (b) adds a linear fit to the mean-variance data, providing more quantitative insights into the detector's characteristics. The slope of this linear fit represents the inverse of the gain of the detector, calculated to be approximately $9.7 \times 10^{-4} \pm 4.5 \times 10^{-5}$ e-/ADU. This gain describes how many electrons correspond to one Analog-to-Digital Unit (ADU) in the camera's output. The intercept of the fit, approximately $0.24 \pm 1 \times 10^{-4}$ ADU, represents the read noise of the detector.

The scatter plot of mean pixel intensity versus variance shows a positive correlation, where the variance increases with the mean pixel intensity. This behavior aligns with the expected Poisson statistics, where the variance in the number of photons detected by a sensor increases with the mean number of photons. At low signal levels, the variance remains relatively small, but as the mean pixel intensity increases, the variance grows linearly. This demonstrates that the fluctuations in pixel intensity (noise) increase with higher light levels. The linearity in this relationship is indicative of a well behaved detector, where the noise increases predictably with the signal. It is also noticeable that the variance is not zero when the signal is zero due to read noise, which is the electronic noise introduced by the detector itself. Even when no photons are detected (no light is present), the detector electronics produce some baseline noise. This noise originates from various processes inside the camera, such as converting the charge accumulated in each pixel to a digital value. At higher signal levels, the relationship between the mean and variance begins to deviate from strict linearity. The variance does not increase as rapidly with the mean as it does at lower intensities. This deviation can be due to several factors, including saturation effects or other non linearity in the detector. As the signal increases, the detector approaches its capacity to measure additional light, which

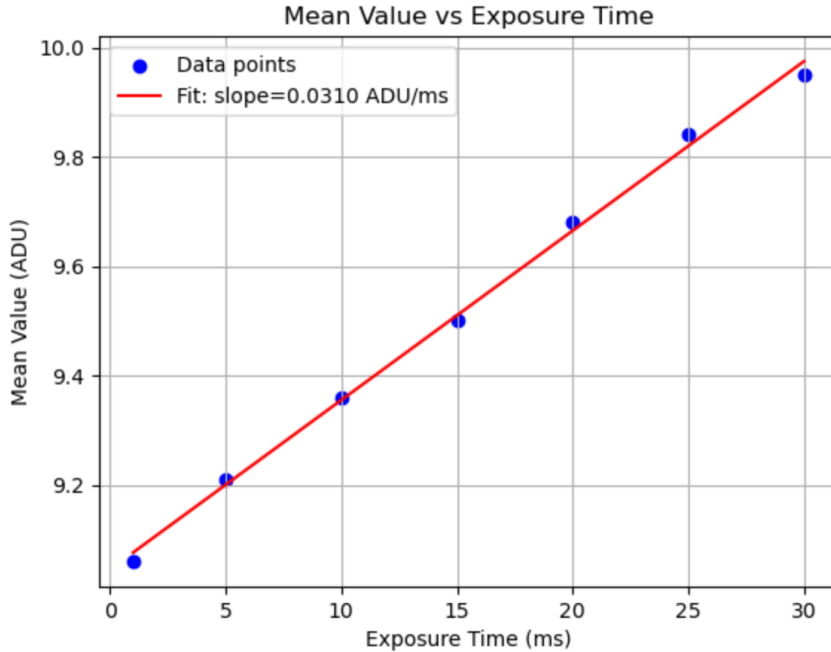


Figure 5: Mean pixel value as a function of exposure time for dark frames. The data points (blue) show a linear relationship, with the slope of the fit (red line) equal to $\pm 7 \times 10^{-4}$ ADU/ms. This slope represents the rate of dark current accumulation in the detector, indicating that the mean pixel value increases steadily with longer exposure times due to thermally generated electrons. The intercept at $9 \pm 7 \times 10^{-2}$ ADU reflects the baseline read noise when the exposure time is near zero.

results in a flattening of the variance. The slope of the linear fit in the mean vs. variance plot is actually $1/gain$ of the detector, not the gain directly. In this case, the slope is 9.7×10^{-4} e-/ADU meaning that the gain of the detector is $1019.9246 \times 10^{-4} \pm 45.9$ e-/ADU. This gain value tells us how many ADUs correspond to a single electron detected by the sensor. A higher gain value (ADU/e-) means the detector is less sensitive and it requires more electrons to produce a significant output in ADUs.

The next important measurement is the dark current of the detector, which was determined from the data shown in Figure 5. This plot displays the mean pixel intensity as a function of exposure time for dark frames, where no external light is incident on the detector. As expected, the mean pixel intensity increases linearly with the exposure time which indicates that dark current, caused by thermally generated electrons within the detector, accumulates over time. The slope of the linear fit is $0.031 \pm 7 \times 10^{-4}$ ADU/ms, which gives the rate at which dark current is building up in the detector. By multiplying the slope by 1000, the

dark current is found to be approximately 31 ADU/sec/pixel. To convert this value to electrons per second per pixel, we can divide by the detector gain, which was previously calculated to be $1019.9246 \times 10^{-4} \pm 45.9$ e-/ADU. The resulting dark current is approximately 28.9 ± 0.1 e-/sec/pixel. This value represents the rate at which thermal noise accumulates in each pixel of the detector over time, even in the absence of light. The intercept of the fit, reflects the baseline noise level of the detector when the exposure time is near zero. This is likely a combination of read noise as well as any residual electronic noise present in the system.

5 Discussion & Conclusion

The results of this experiment provide valuable insights into the performance of the Point Grey FMVU-03MTM-CS CMOS detector, specifically in terms of photon noise, detector gain, and dark current accumulation. By analyzing the relationship between mean pixel intensity and variance, the key metrics were determined, such as the detector's gain of approximately $1019.9246 \times 10^{-4} \pm 45.9$ e-/ADU and a dark current of 28.9 ± 0.1 e-/sec/pixel. The low gain highlights the detector's high sensitivity, which is ideal for capturing faint signals in low-light conditions. Additionally, the read noise was measured as $0.34 \pm 1 \times 10^{-4}$ ADU which represents the minimum detectable signal level due to electronic noise in the system.

The experiment confirmed that at lower signal levels, the detector followed Poisson statistics, with the variance increasing proportionally with the mean pixel intensity, consistent with photon-counting systems. However, at higher signal levels, the relationship between mean and variance plateaued, likely due to saturation effects or other non-Poisson noise sources, indicating the detector's limitations at high intensities. This behavior is also important to understanding the detector's performance in different imaging scenarios, as high-intensity signals can impact the quality of data collected.

The measurement of dark current, which increases linearly with exposure time, is particularly important in long exposure imaging. With a dark current of approximately 28.9 ± 0.1 e-/sec/pixel, the detector exhibits significant noise accumulation over time, which must be corrected for in low-light imaging applications, especially in fields such as astronomy, where long exposures are common. By quantifying and correcting for this noise, we ensure the accuracy of measurements and improve the detector's reliability in real-world applications.

This experiment also emphasizes the importance of noise correction techniques, such as dark frame subtraction, and highlights the need for precise calibration in scientific imaging. The findings from this experiment are applicable to a wide range of fields that rely on accurate photon detection such as astronomy to microscopy. Future work could focus on reducing dark current through temperature control or even improving pixel uniformity. Overall, this experiment forms a base for further understanding and optimizing CMOS detectors in precision imaging, ensuring accurate and reliable data collection in

future applications.

6 Bibliography

Department of Astronomy and Astrophysics, *Basic Photon Statistics: Lab Manual for AST325/326 (Fall 2024)*, University of Toronto, September 2024.

Appendix:

6.0.1 Code to calculate mean and standard deviation

```
1 # defining custom functions for mean and standard deviation
2 def my_mean(data):
3     return sum(data) / len(data)
4
5 def my_std(data):
6     mean = my_mean(data)
7     variance = sum((x - mean) ** 2 for x in data) / len(data)
8     return variance ** 0.5
```

Listing 1: Python code for calculating the mean and standard deviation of a dataset.

Listings

- | | | |
|---|--|----|
| 1 | Python code for calculating the mean and standard deviation of
a dataset. | 12 |
|---|--|----|